Robust Control of a Hard Disk Drive

Università degli Studi di Pisa

Information Engineering Department

Master's Degree in Robotics and Automation Engineering

Control of Uncertain Systems course project

Di Luzio Fulvio

492897

fulvio.diluzio@gmail.com

Contents

1 Introduction **3**

2 Course project **3**

3 H_∞ and μ general concepts **3**

3.1 General H_∞ Control . . . 3

3.2 μ Analysis and Synthesis . . . 4

4 Hard Disk Drive Servo System **5**

4.1 Derivation of Uncertainty Model . . . 7

4.2 Closed-loop System Design Specifications . . . 7

4.3 System Specifications . . . 9

4.4 Model Transfer Function . . . 9

4.5 Weighting Functions . . . 9

5 Controllers **11**

5.1 *μ Controller* . . . 11

5.2 *H_∞ Controller* . . . 13

5.3 *LQG Controller* . . . 15

5.4 *PID Controller* . . . 16

6 Controllers comparison **18**

6.1 Frequency response of the controllers . . . 18

6.2 Frequency response of the closed-loop systems . . . 19

6.3 Transient response of the closed-loop systems . . . 19

6.4 Nominal Performance . . . 20

6.5 Robust Stability . . . 21

6.6 Robust Performance . . . 21

7 GUI **22**

A Matlab files **23**

List of Figures

1 P-K structure. 3
2 Block diagram of the closed-loop system for μ analysis and synthesis. 4
3 Schematic diagram of a hard disk drive. 5
4 Block diagram of the hard disk drive servo system. 6
5 Plant model in the form of an upper LFT. 7
6 Block diagram of the closed-loop system with performance specifications. 7
7 Frequency response of the ideal model M. 9
8 Frequency response of the noise shaping function. 10
9 Frequency response of the inverse of W_p. 10
10 Frequency response of the three control weighting functions. 11
11 Block diagram of the closed-loop system with μ controller. 11
12 RS and RP for the first μ controller. 12
13 Closed-loop system with H_∞ controller. 14
14 RS and RP for the H_∞ controller. 14
15 Closed-loop system with LQG controller. 15
16 Closed-loop system with PID controller. 17
17 RS and RP for the PID controller. 17
18 Comparison of the controllers frequency response. 18
19 Comparison of the frequency closed-loop systems. 19
20 Comparison of the output sensitivities. 19
21 Comparison of the transient responses of the closed-loop systems. 19
22 Comparison of the control actions. 20
23 Nominal performance of the closed-loop systems. 20
24 Robust stability of the closed-loop systems. 21
25 Robust performance of the closed-loop systems. 21
26 Graphic User Interface. 22

1 Introduction

This report shows the developed work for the *Control of Uncertain Systems* course project. The paper is organized as follows. Section 2 explains the project goals. In Section 3 μ and H_∞ controllers are briefly explained. Section 4 provides information about the system of a Hard Disk Driver (HDD). Section 6 illustrates the designed controllers. In Section 6 a comparison between controllers is shown. Section 7 shows the designed GUI. Finally, an appendix with all the Matlab file is presented.

2 Course project

The goal of this work project is the design of a robust servo system of *hard disk drive*(HDD), with the use of the software $Matlab$ (v. **R2016b**). Four designed controllers are applied, namely μ-controller, H_∞, LQG and PID. These controllers are compared in aspects of robustness of closed-loop system stability and of performance in the frequency domain and in the time-domain.

3 H_∞ and μ general concepts

3.1 General H_∞ Control

Given the control system in Figure 1 and the partition of $P(s)$,

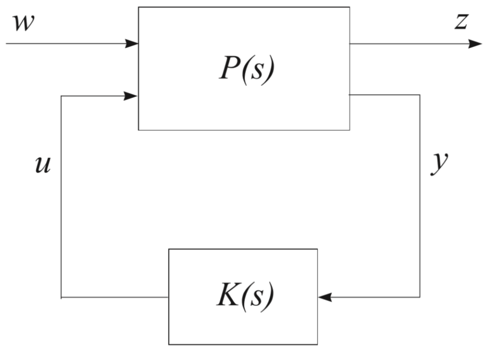

$$\text{P(s)} = \begin{bmatrix} P_{zw} & P_{zu} \\ P_{yw} & P_{yu} \end{bmatrix}$$

Figure 1: P-K structure.

The closed-loop system is given by the transfer matrix

$$F[P(s), K(s)] = T_{zw}(s) = P_{zw} + P_{zu}K(I - P_{yu}K)^{-1}P_{yw}$$

Then, the H_∞ optimal control problem consists in finding a causal controller $K(s)$ which stabilizes $P(s)$ and which minimizes the cost function

$$J_\infty(K) = \|F[P(s), K(s)]\|_\infty = \|T_{zw}(s)\|_\infty = \sup_{\omega \in \mathbf{R}} \sigma_{max}[T_{zw}(j\omega)]$$

However, the minimization of $J_\infty(K)$ is a very hard problem. Therefore conditions to ensure the existence of a stabilizing controller have been found, such that the H_∞-norm bound holds for a given $\gamma > \gamma_{min} > 0$:

$$J_\infty(K) < \gamma, \quad where \quad \|T_{zw}(s)\|_\infty := \sup_{\omega \in \mathbf{R}} \sigma_{max}[T_{zw}(j\omega)] = \gamma_{min}$$

The procedure to find $\gamma > \gamma_{min} > 0$ is called $\gamma - iteration$ and lets to find γ with any degree of accuracy.

3.2 μ Analysis and Synthesis

The quest is to develop a general procedure for the synthesis of a robust controller, with respect to structured and unstructured uncertainties, that can verity and guarantee stability and performance.

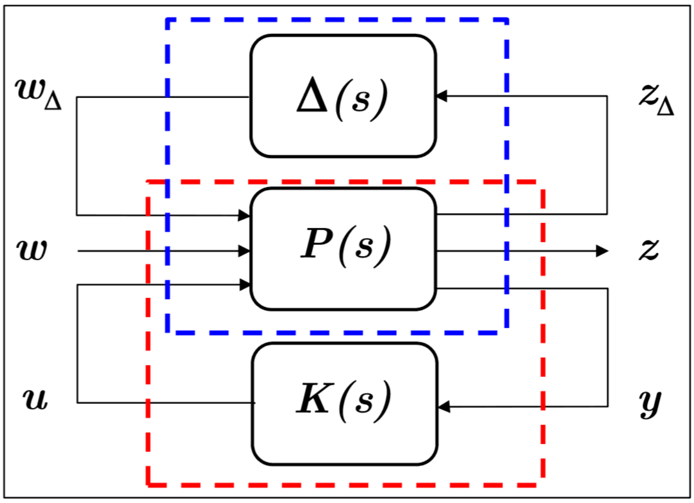

Figure 2: Block diagram of the closed-loop system for μ analysis and synthesis.

Robustness Synthesis is a 2 - Block representation, which includes the uncertainty structure in $G(s)$:

$$\begin{bmatrix} z \\ y \end{bmatrix} = G(s) \begin{bmatrix} w \\ u \end{bmatrix}$$

$$G(s) = \begin{bmatrix} G_{11}(s) & G_{12}(s) \\ G_{21}(s) & G_{22}(s) \end{bmatrix}$$

$$G_{zw}(s) = F_L\{G(P, \Delta), K\}$$

It means to find $K(s)$ to obtain robustness.

Robust Analysis is a 2 - Block representation, which includes the closed-loop controller in $N(s)$:

$$\begin{bmatrix} z_\Delta \\ yz \end{bmatrix} = N(s) \begin{bmatrix} w_\Delta \\ w \end{bmatrix}$$

$$N(s) = \begin{bmatrix} N_{11}(s) & N_{12}(s) \\ N_{21}(s) & N_{22}(s) \end{bmatrix}$$

$$N_{zw}(s) = F_U\{N(P, K), \Delta\}$$

It means, given $K(s)$, verify where robustness is obtained.

Robust Stability: The controller $K(s)$, within the feedback $N(s)$ stabilises the normal system (i.e. when $\Delta = 0$) as well as the closed-loop uncertain 2 - Block structure, for all the uncertainties assumed in Δ.

The critical relationship for robust stability is that, given

$$z = N_{22} + N_{21}\Delta(I - M\Delta)^{-1}N_{12} \qquad N_{11}(s) = M(s)$$

$I - M\Delta$ has to be stable and invertible.

In order to verify robustness, a parameter r is introduced, which shrinks or expands the set Δ. Then we must determine the biggest $r*$ such that

$$det[I - M\Delta] \neq 0 \quad \forall\Delta \in r\Delta$$

The **structured singular value** of the complex matrix $M(s)$, with respect to Δ, is defined as:

$$\mu_\Delta = \frac{1}{sup\{r|det(I - M\Delta) \neq 0, \forall\Delta \in r\Delta\}}$$

It can be shown that $I - M\Delta$ has a proper and stable inverse if $\mu_\Delta \leq 1$. Therefore, the lower the value of μ_Δ, the biggest the set Δ for which robustness is guaranteed.

$\mu[M(s)]$ is frequency dependent and so it should be calculated for each frequency over a certain range. The computation of the structured singular value is a hard problem. Therefore in practice, based on some properties of μ, its upper and lower bounds can be calculated. It is possible to demonstrate that

$$\rho(M) \leq \mu_\Delta(M) \leq \sigma_{max}(M)$$

So the lower bound of μ is given by the *spectral radius* $\rho(M)$, while the upper bound is given by the *maximum singular value* $\sigma_{max}(M)$.

The numerical procedure to compute the upper bound is called **D-K iteration**. Given scaling matrices on $M(s)$ and a controller $K(s)$, the iteration reduces the value of μ until it cannot be decreased any more. The procedure make use of a cost function in order to minimise the controller $K(s)$.

4 Hard Disk Drive Servo System

A hard disk drive is a data storage device that uses magnetic storage to store and retrieve digital information. The schematic diagram of a typical hard disk drive is shown in Figure 3.

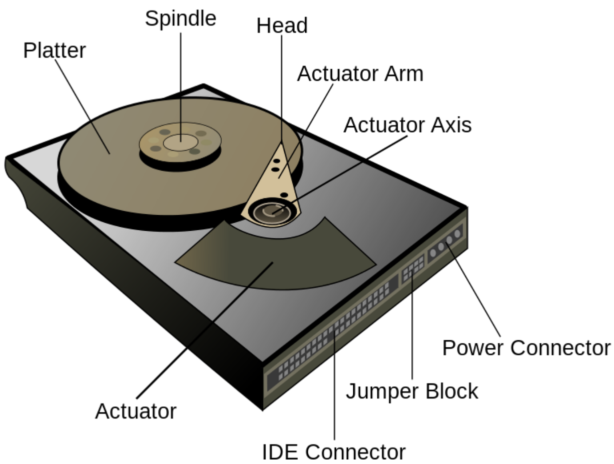

Figure 3: Schematic diagram of a hard disk drive.

The disk assembly consists of several flat disks called *platters* coated on both sides with very thin layer of magnetic material (thin film media). The magnetic material is used to store the data in the form of magnetic patterns. The data are retrieved from, or recorded onto, the platters by electromagnetic *read*/*write*(R/W) heads which are mounted at the bottom of *sliders*. These sliders are mounted onto head arms and move rapidly on the platter surface. The data recorded on the platters are in concentric circles called *tracks*. The head arms are moved on the surface of the platter by a rotary voice coil actuator called *Voice Coil Motor*(VCM). By controlling the current in the coil, the heads can move in one direction or the other in order to follow precisely the data track.

The goal of the hard disk drive servo control system is to achieve a precise positioning of the read/write heads on the desired track (track following mode).

The block-diagram of the HDD servo system is shown in Figure 4.

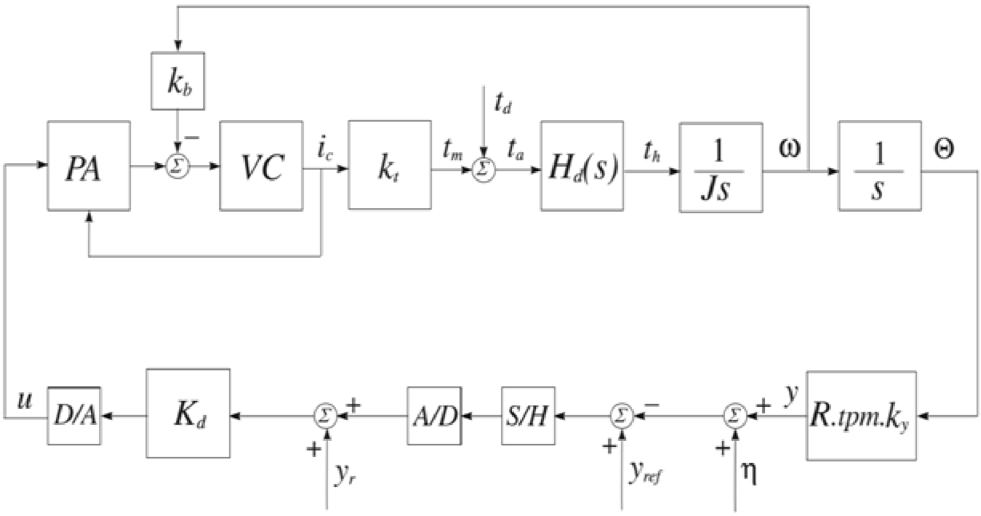

Figure 4: Block diagram of the hard disk drive servo system.

- VCM: the Voice Coil Motor driven by the output current ic;
- k_t: VCM torque constant;
- $H_d(s)$: actuator mechanical resonant modes;
- ω: angular velocity;
- J: arm moment of inertia;
- θ: angle of arm rotation;
- k_y: position measurement gain;
- R: arm length;
- tpm: tracks per meter;
- y: position signal;
- η: position noise signal;
- y_{ref}: reference signal;
- K_d: servo controller;
- u: control signal.

4.1 Derivation of Uncertainty Model

The uncertainties taken into account are all structured and the main ones are related to: the variations in the frequency ω and the damping coefficient ξ of the mechanical resonant modes; the rigid body parameters, i.e. k_t, J, k_y. They are represented as follows:

$$\omega = \bar{\omega}(1 + p_\omega \delta_\omega) \quad \xi = \bar{\xi}(1 + p_\xi \delta_\xi)$$
$$k_t = \bar{k_t}(1 + p_{k_t} \delta_{k_t}) \quad J = \bar{J}(1 + p_J \delta_J) \quad k_y = \bar{k_y}(1 + p_{k_y} \delta_{k_y})$$

where $\bar{x}$ is the nominal value, p_x the maximum relative uncertainty and $\delta_x \in$ [-1,1].

All the uncertainties can be gathered in one block Δ:

$$\Delta = diag(\delta_{\omega_1}, \delta_{\omega_1}, \delta_{\xi_1}, \delta_{\omega_2}, \delta_{\omega_2}, \delta_{\xi_2}, \delta_{\omega_3}, \delta_{\omega_3}, \delta_{\xi_3}, \delta_{\omega_4}, \delta_{\omega_4}, \delta_{\xi_4}, \delta_{k_t}, \delta_J, \delta_{k_y})$$

A perturbed plant model in the form of an upper LFT $F_U(Gnom, \Delta)$ can be obtained and shown in figure 5.

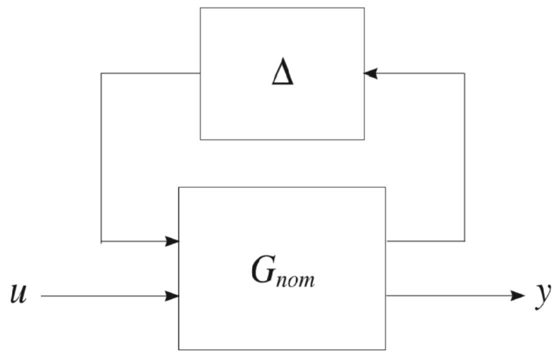

Figure 5: Plant model in the form of an upper LFT.

4.2 Closed-loop System Design Specifications

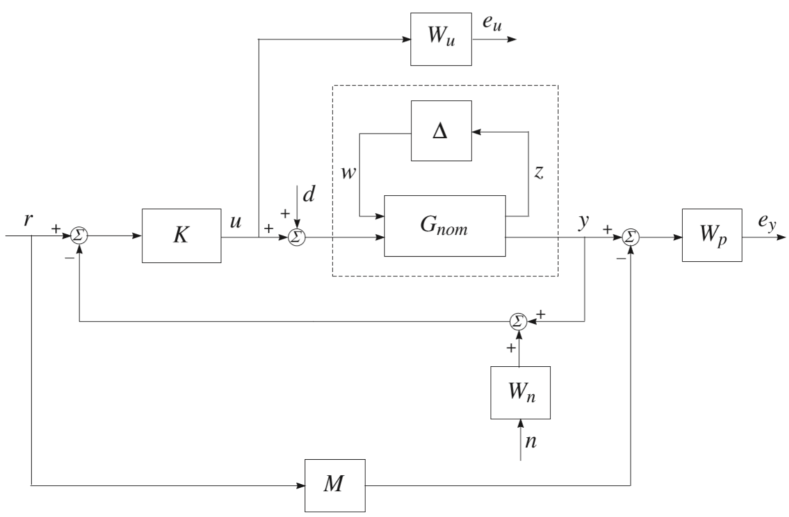

Figure 6: Block diagram of the closed-loop system with performance specifications.

Figure 6 shows the block diagram of the closed-loop system, which includes the feedback structure and the controller as well as the elements representing the model uncertainty and the performance objectives. W_n is a weighting function that shapes the noise signal. The transfer

matrices W_p and W_u are used to reflect the relative significance of the different frequency ranges for which the performance is required. M is an ideal model of performance, to which the designed closed loop system tries to match.
Hence, the performance objective can be recast, with possible slight conservativeness, as that the $\|\cdot\|_\infty$ of the transfer function matrix from r, d and n to e_y and e_u is less than 1.

$$\begin{bmatrix} e_y \\ e_u \end{bmatrix} = \begin{bmatrix} W_p(S_oGK - M) & W_pS_oG & -W_pS_oGKW_n \\ W_uS_iK & -W_uKS_oG & -W_uKS_oW_n \end{bmatrix} \begin{bmatrix} r \\ d \\ n \end{bmatrix}$$

where $S_i = (I+GK)^{-1}$ and $S_o = (I+KG)^{-1}$ are, respectively, the input and output sensitivities. The six functions to be minimised are described in Table 1.

Function	***Description***
$W_p(S_oGK - M)$	Weighted difference between the ideal and actual closed-loop systems
W_pS_oG	Weighted disturbance sensitivity
$W_pS_oGKW_n$	Weighted noise sensitivity
W_uS_iK	Weighted control effort due to reference
W_uKS_oG	Weighted control effort due to disturbance
$W_uKS_oW_n$	Weighted control effort due to noise

Table 1: H_∞ functions to be minimized.

The controller synthesis problem of the Hard Disk Drive Servo System is to find a linear, output feedback controller $K(s)$ which has to ensure the following properties of the closed-loop system.

Nominal Performance

The closed-loop system achieves nominal performance if the performance objective is satisfied for the nominal plant model.

$$\left\| \begin{bmatrix} W_p(S_oG_{nom}K - M) & W_pS_oG_{nom} & -W_pS_oG_{nom}KW_n \\ W_uS_iK & -W_uKS_oG_{nom} & -W_uKS_oW_n \end{bmatrix} \right\|_\infty < 1$$

Robust Stability

The closed-loop system achieves robust stability if the closed-loop system is internally stable for each possible plant dynamics $G = F_U(G_{nom}, \Delta)$.

Robust Performance

The closed-loop system must remain internally stable for each $G = F_U(Gnom, \Delta)$ and in addition the performance criterion

$$\left\| \begin{bmatrix} W_p(S_oG_{nom}K - M) & W_pS_oG_{nom} & -W_pS_oG_{nom}KW_n \\ W_uS_iK & -W_uKS_oG_{nom} & -W_uKS_oW_n \end{bmatrix} \right\|_\infty < 1$$

should be satisfied for each $G = F_U(Gnom, \Delta)$.

4.3 System Specifications

The following constraints have to be respected:

- Peak closed-loop gain $< 4\ dB$
- Open-loop gain $> 20\ dB$ at $100\ Hz$
- Steady state error $< 0.1\ \mu m$
- Settling time $< 1.5\ ms$
- Closed-loop bandwidth $> 1000\ Hz$
- Gain Margin $> 5\ dB$
- Phase margin $> 40\ deg$

In addition, it is necessary to have control action smaller than $1.2\ V$, in order to avoid the power amplifier saturation, and good disturbance rejection and noise attenuation.

4.4 Model Transfer Function

The model transfer function is chosen so that the time response to the reference signal would have an overshoot less than 20 % and a settling time less than $1\ ms$.

$$M = \frac{1}{3.75 \times 10^{-9} s^2 + 1.2 \times 10^{-4} s + 1}$$

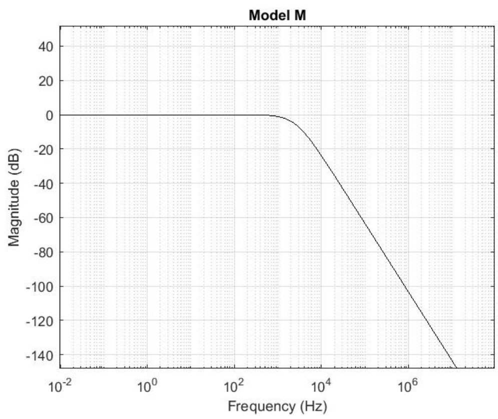

Figure 7: Frequency response of the ideal model M.

4.5 Weighting Functions

The noise weighting function W_n is determined on the basis of the spectral density of the position noise signal, whose spectral content is usually above $500\ Hz$.

$$W_n = 6 \times 10^{-4} \frac{0.1s + 1}{0.001s + 1}$$

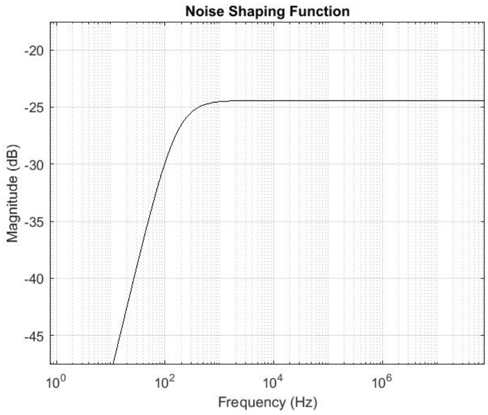

Figure 8: Frequency response of the noise shaping function.

The closed-loop system performance specifications are reflected by the weighting performance function $W_p(s)$. Three performance weighting functions are considered in the design.

$$W_{p1}(s) = 10^-4 \frac{s^2 + 8 \times 10^4 s + 10^8}{s^2 + 7 \times 10^4 s + 2.5 \times 10^4}$$

$$W_{p2}(s) = 10^-4 \frac{s^2 + 4 \times 10^5 s + 2.5 \times 10^9}{s^2 + 3.9 \times 10^5 s + 6.25 \times 10^5}$$

$$W_{p3}(s) = 10^-4 \frac{s^2 + 1.15 \times 10^6 s + 10^{10}}{s^2 + 1.05 \times 10^6 s + 9 \times 10^6}$$

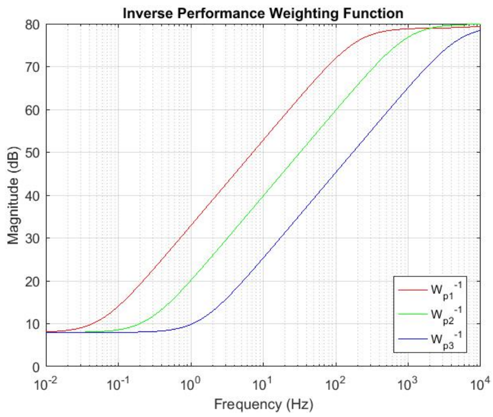

Figure 9: Frequency response of the inverse of W_p.

The control weighting function is usually chosen as high pass filter in order to ensure that the control action will not exceed 1.2 V. Again, three weighting functions are considered in the design.

$$W_{u1}(s) = 10^{-6} \frac{0.385 s^2 + s + 1}{10^{-4} s^2 + 2 \times 10^{-3} s + 1}$$

$$W_{u2}(s) = 10^{-6} \frac{0.55 s^2 + s + 1}{10^{-4} s^2 + 2.1 \times 10^{-3} s + 1}$$

$$W_{u3}(s) = 3 \times 10^{-6} \frac{4.05 s^2 + s + 1}{10^{-4} s^2 + 2 \times 10^{-3} s + 1}$$

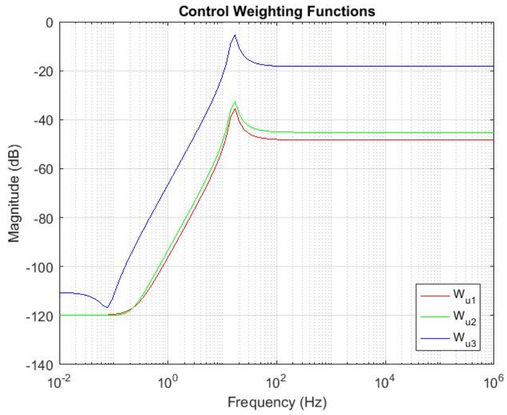

Figure 10: Frequency response of the three control weighting functions.

Those three control weighting functions W_u are paired with the three performance weighting functions W_p, in the given order, in the μ-synthesis.

5 Controllers

5.1 μ *Controller*

In the μ-synthesis only the inputs and outputs of the uncertainty in the rigid body model (i.e., the parameters k_t, J and k_y) will be considered. The inclusion of the uncertainties of resonant modes would make the D-K iterations difficult to converge.

The block diagram of the closed loop system used in the μ synthesis is shown in Figure 11.

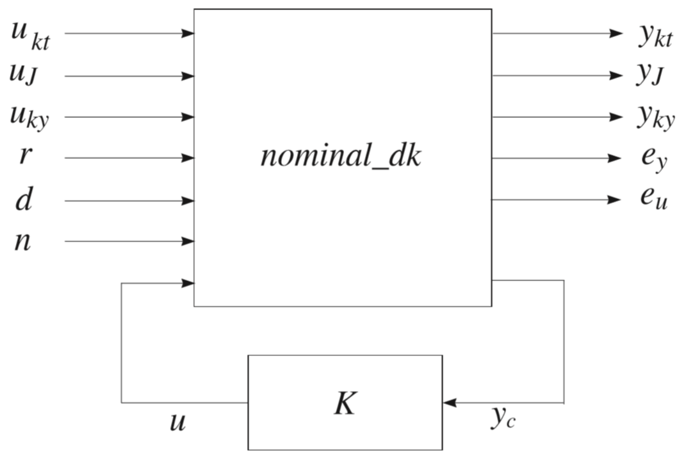

Figure 11: Block diagram of the closed-loop system with μ controller.

Denote by $P(s)$ the transfer matrix of the seven-input, six-output, open-loop system **nominal_dk** and let the block structure of the uncertainty Δ_P be defined as

$$\Delta_P := \left\{ \begin{bmatrix} \Delta_r & 0 \\ 0 & \Delta_F \end{bmatrix} : \Delta_r \in \mathbf{R}^{3\times 3}, \Delta_F \in \mathbf{C}^{3\times 2} \right\}$$

The first block of this uncertainty matrix corresponds to the block Δ_r containing the uncertainties in the rigid body model, while the second block Δ_F is a fictitious uncertainty block which is used for the performance requirements in the μ approach.

To guarantee robust performance, it needs to find a stabilising controller $K(s)$ such that, for each frequency $\omega \in [0, \infty]$, the following holds:

$$\mu_{\Delta_P}[F_L(P,K)(j\omega)] < 1$$

The fulfilment of this condition guarantees robust performance of the closed-loop system, i.e.

$$\left\| \begin{bmatrix} W_p(S_oGK - M) & W_pS_oG & -W_pS_oGKW_n \\ W_uS_iK & -W_uKS_oG & -W_uKS_oW_n \end{bmatrix} \right\|_\infty < 1$$

The μ controller is designed three times, each time with the corresponding weighting functions pair (i.e. W_p and W_u). The results for robust stability and robust performance analysis are shown in Table 2. In each case six DK iteration are used.

Controller	***Order***	***Robust Stability*** μ_{max}	***Robust Performance*** μ_{max}
1	38	0.37296	0.43625
2	38	0.41163	0.54945
3	26	0.34509	1.9333

Table 2: Robust stability and robust performance for the three μ controllers.

The closed-loop system achieves robust stability and robust performance in each case, but the third corresponding to the pair (W_{p3},W_{u3}). In terms of gain and phase margins, the best controller is the first one, as shown in Table 3.

Controller	***Gain margin*** dB	***Phase margin*** deg
1	10.9009	59.0071
2	9.838	50.9925
3	-10.4504	36.3051

Table 3: Gain and phase margins for the three μ controllers.

Since the best controller is the first one, the graphics of robust stability and robust performance relative to it are reported in Figures 12.a and 12.b.

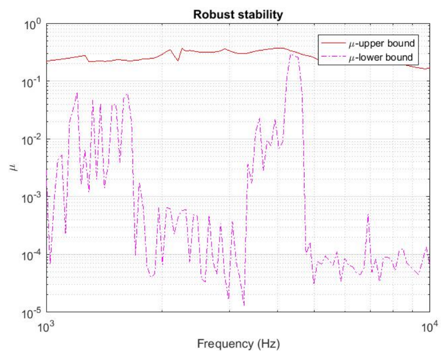

(a) Robust Stability.

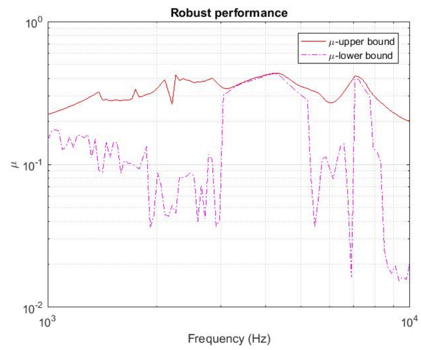

(b) Robust Perfomance.

Figure 12: RS and RP for the first μ controller.

Then, the performance specifications are illustrated.

Specification	***Constraint***	***Value***
Peak closed-loop gain	$< 4\ dB$	$2.04\ dB$
Open-loop gain	$> 20\ dB$ at $100\ Hz$	$29.39\ dB$
Steady state error	$<0.1\ \mu m$	$0\ \mu m$
Settling time	$< 1.5\ ms$	$1.6\ ms$
Closed-loop bandwidth	$> 1000\ Hz$	$1060\ Hz$
Gain margin	$> 5\ dB$	$10.9009\ dB$
Phase margin	$> 40\ deg$	$59.0071\ deg$
Max control action	$< 1.2\ V$	$1.193\ V$
Overshoot	$< 20\ \%$	$20.356\ \%$

Table 4: Specifications due to the first μ controller.

And the following results:

- *Disturbance error*: 28.7598 %
- *Noise error*: 1.3673 %

All the constraints are respected, but the settling time (even if for a bit).

Finally, zeros and pole of the controller are shown.

Zeros

1.0e+05 *

-1.5958 + 0.0000i	-0.7048 + 0.0000i
-0.7000 + 0.0000i	-0.4216 + 0.0000i
-0.0942 + 0.5451i	-0.0942 - 0.5451i
-0.0363 + 0.4004i	-0.0363 - 0.4004i
-0.0951 + 0.4059i	-0.0951 - 0.4059i
-0.0710 + 0.3931i	-0.0710 - 0.3931i
-0.3193 + 0.0635i	-0.3193 - 0.0635i
-0.0035 + 0.1380i	-0.0035 - 0.1380i
-0.1405 + 0.0000i	-0.1600 + 0.0327i
-0.1600 - 0.0327i	-0.1005 + 0.0000i
-0.0687 + 0.0000i	-0.0666 + 0.0000i
-0.0337 + 0.0000i	-0.0158 + 0.0000i
-0.0144 + 0.0000i	-0.0100 + 0.0000i
-0.0085 + 0.0052i	-0.0085 - 0.0052i
-0.0047 + 0.0000i	-0.0031 + 0.0000i
-0.0009 + 0.0030i	-0.0009 - 0.0030i
-0.0003 + 0.0000i	-0.0001 + 0.0001i
-0.0001 - 0.0001i	-0.0001 + 0.0010i
-0.0001 - 0.0010i	

Poles

1.0e+05 *

-0.6970 + 0.0085i	-0.6970 - 0.0085i
-0.7000 + 0.0000i	-0.4467 + 0.3510i
-0.4467 - 0.3510i	-0.0886 + 0.5522i
-0.0886 - 0.5522i	-0.4049 + 0.0000i
-0.0677 + 0.4427i	-0.0677 - 0.4427i
-0.0718 + 0.3961i	-0.0718 - 0.3961i
-0.0950 + 0.4061i	-0.0950 - 0.4061i
-0.3228 + 0.0766i	-0.3228 - 0.0766i
-0.0035 + 0.1389i	-0.0035 - 0.1389i
-0.1458 + 0.0000i	-0.0712 + 0.0000i
-0.1600 + 0.0327i	-0.1600 - 0.0327i
-0.0668 + 0.0000i	-0.0346 + 0.0000i
-0.0165 + 0.0000i	-0.0129 + 0.0000i
-0.0100 + 0.0000i	-0.0047 + 0.0000i
-0.0031 + 0.0000i	-0.0009 + 0.0030i
-0.0009 - 0.0030i	-0.0000 + 0.0010i
-0.0000 - 0.0010i	-0.0003 + 0.0000i
-0.0000 + 0.0000i	-0.0001 + 0.0001i
-0.0001 - 0.0001i	-1.5750 + 0.0000i

5.2 H_∞ *Controller*

The aim of the design in this case is to find an $H_\infty(sub)$optimal, output controller for the interconnection shown in Figure 13 in which the inputs and outputs of the uncertainty block are excluded.

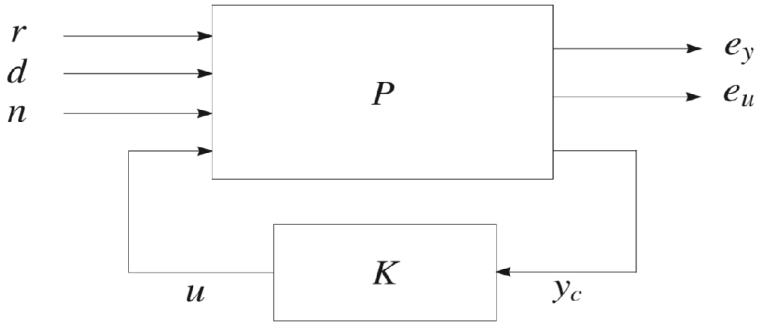

Figure 13: Closed-loop system with H_∞ controller.

Here the optimal control minimises the $\infty-norm$ of $F_L(P,K)$ in respect to the transfer function K of the controller. $F_L(P,K)$ is the nominal close-loop transfer function matrix.

The controller obtained is of 18th order and guarantees robust stability and robust performance as shown in the following Table and Figures.

Order	***Robust Stability*** μ_{max}	***Robust Performance*** μ_{max}
18	0.43293	0.48774

Table 5: Robust stability and robust performance for the H_∞ controller.

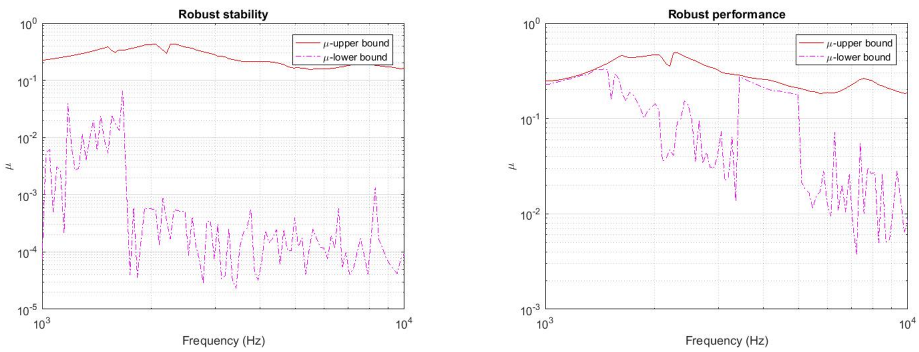

(a) Robust Stability.

(b) Robust Perfomance.

Figure 14: RS and RP for the H_∞ controller.

Then, the performance specifications are illustrated.

Specification	***Constraint***	***Value***
Peak closed-loop gain	$< 4\ dB$	$4.895\ dB$
Open-loop gain	$> 20\ dB$ at $100\ Hz$	$35.88\ dB$
Steady state error	$<0.1\ \mu m$	$0\ \mu m$
Settling time	$< 1.5\ ms$	$1.87\ ms$
Closed-loop bandwidth	$> 1000\ Hz$	$1500\ Hz$
Gain margin	$> 5\ dB$	$12.4245\ dB$
Phase margin	$> 40\ deg$	$36.187\ deg$
Max control action	$< 1.2\ V$	$0.789\ V$
Overshoot	$< 20\ \%$	$48.8677\ \%$

Table 6: Specifications due to H_∞ controller.

And the following results:

- *Disturbance error*: 22.0619 %
- *Noise error*: 1.2401 %

All the constraints are met, but overshoot and phase margin.

Finally, zeros and pole of the controller are shown.

Zeros

1.0e+04 *

-7.0000 + 0.0000i	-0.9566 + 5.4456i
-0.9566 - 5.4456i	-0.5184 + 3.9866i
-0.5184 - 3.9866i	-0.0332 + 1.3818i
-0.0332 - 1.3818i	-1.6000 + 0.3266i
-1.6000 - 0.3266i	-1.0070 + 0.0000i
-0.1000 + 0.0000i	-0.1523 + 0.0486i
-0.1523 - 0.0486i	-0.0094 + 0.0301i
-0.0094 - 0.0301i	-0.0010 + 0.0099i
-0.0010 - 0.0099i	

Poles

1.0e+04 *

-2.1114 + 6.7364i	-2.1114 - 6.7364i
-7.0000 + 0.0000i	-4.9215 + 2.7203i
-4.9215 - 2.7203i	-2.7459 + 0.0000i
-0.8261 + 4.9147i	-0.8261 - 4.9147i
-1.6000 + 0.3266i	-1.6000 - 0.3266i
-0.1000 + 0.0000i	-0.0329 + 1.3904i
-0.0329 - 1.3904i	-0.0004 + 0.0101i
-0.0004 - 0.0101i	-0.0000 + 0.0000i
-0.0094 + 0.0301i	-0.0094 - 0.0301i

5.3 *LQG Controller*

The $Linear-Quadratic-Gaussian$ (LQG) regulator is the combination of a $Kalman\ filter$, i.e. a $Linear-Quadratic-Estimator$ (LQE), with a $Linear-Quadratic-Regulator$ (LQR). LQG optimality does not automatically ensure good robustness properties. The robust stability of the closed loop system must be checked separately after the LQG controller has been designed. The $Loop\ Transfer\ Recovery$ method (LTR) is a modification of the LQG controller, where design parameters are changed in order to achieve robustness similar to the LQR (at input) or to the KBF (at output). The LTR approach can be applied only to *minimum phase* systems and that is not the case since the transfer function $P_{yu}(s)$, from the control input u to the output y, has a zero in the right part of the s plane. Therefore a standard LQG has been designed.

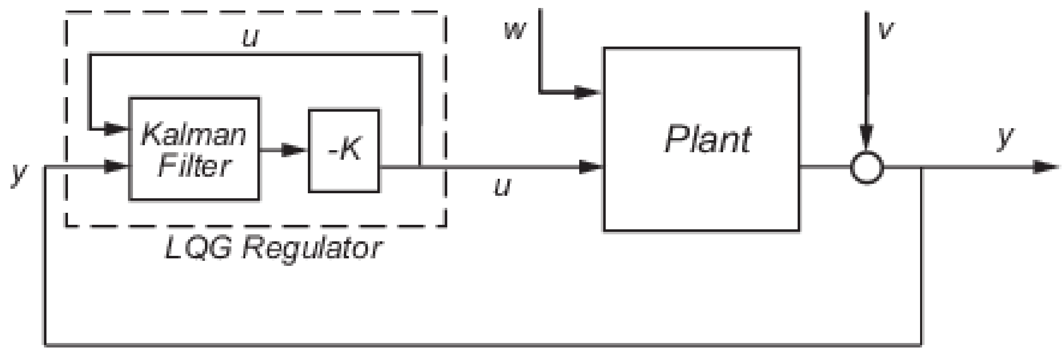

Figure 15: Closed-loop system with *LQG* controller.

The found controller stabilises the nominal plant, but it does not guarantee robust stability and robust performance. The structure singular value analysis gives the result reported in Table 7.

Robust Stability μ_{max}	***Robust Performance*** μ_{max}
74.9181	437.985

Table 7: Robust stability and robust performance for the LQG controller.

Specification	***Constraint***	***Value***
Peak closed-loop gain	< 4 dB	0 dB
Open-loop gain	> 20 dB at 100 Hz	19.3 dB
Steady state error	$<$0.1 μm	0 μm
Settling time	< 1.5 ms	1.93 ms
Closed-loop bandwidth	> 1000 Hz	500 Hz
Gain margin	> 5 dB	13.0669 dB
Phase margin	> 40 deg	64.6897 deg
Max control action	< 1.2 V	0.7131 V
Overshoot	< 20 %	6.6058 %

Table 8: Specifications due to LQG controller.

And the following results:

- *Disturbance error*: 206.2959 %
- *Noise error*: 0.97841 %

Many constraint are not met, specially the disturbance error.
Finally, zeros and pole of the controller are shown.

Zeros

1.0e+04 *

-0.9571 + 5.4472i -0.9571 - 5.4472i
-0.5049 + 3.9992i -0.5049 - 3.9992i
-1.1152 + 0.0000i -0.0251 + 1.3712i
-0.0251 - 1.3712i -0.0222 + 0.0000i
-0.0096 + 0.0301i -0.0096 - 0.0301i

Poles

1.0e+04 *

-2.1808 + 6.1040i -2.1808 - 6.1040i
-0.8469 + 4.6987i -0.8469 - 4.6987i
-3.4657 + 3.1266i -3.4657 - 3.1266i
-4.8938 + 0.0000i -0.0632 + 1.3985i
-0.0632 - 1.3985i -0.0094 + 0.0301i
-0.0094 - 0.0301i

5.4 *PID Controller*

$Proportional - Integral - Derivative$(PID) controllers are very common in industrial sectors due to their simplicity. The general form is the following:

$$C(s) = K_p + \frac{K_i}{s} + \frac{K_d s}{T_f s + 1}$$

where K_p,K_i and K_d denote the *proportional*, *integrative* and *derivative* term, respectively.

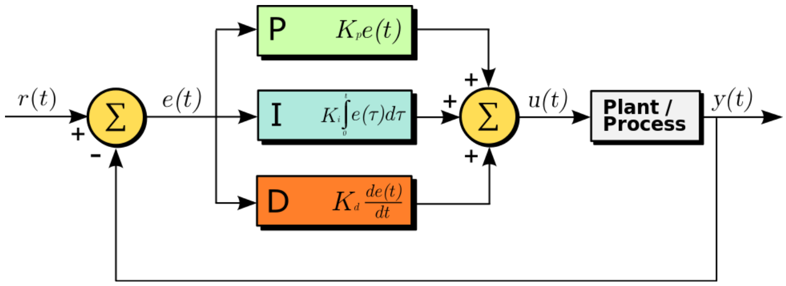

Figure 16: Closed-loop system with PID controller.

As well as in the LQG case, the PID controller is designed respect to the nominal transfer function $P_{yu}(s)$, from the control input u to the output y, and then the structure singular value analysis is applied.

The controller parameters are showed in Table 9.

K_p	K_i	K_d	T_f
0.0132	0.734	8.69e-06	1.45e-05

Table 9: PID controller parameters.

The results of the structured singular value analysis are showed in Table 10.

Robust Stability μ_{max}	***Robust Performance*** μ_{max}
0.45838	0.5429

Table 10: Robust stability and robust performance for the PID controller.

And the relative graphics in Figures 17.a and 17.b.

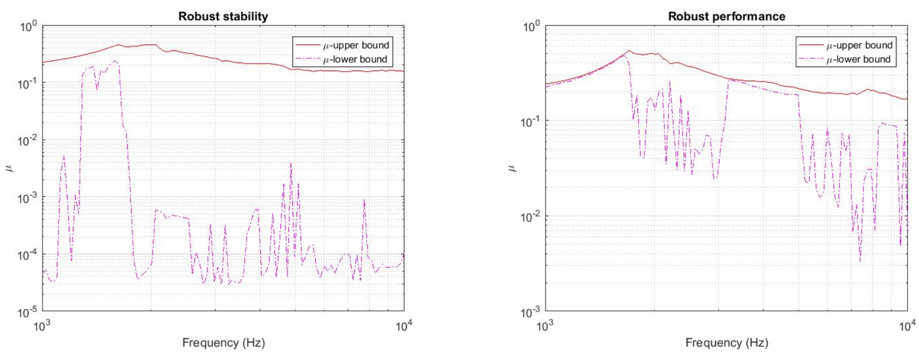

(a) Robust Stability.

(b) Robust Perfomance.

Figure 17: RS and RP for the PID controller.

Therefore, the PID controller guarantees both robust stability and robust performance.

Then, the performance specifications are illustrated.

Specification	*Constraint*	*Value*
Peak closed-loop gain	$< 4\ dB$	$3.945\ dB$
Open-loop gain	$> 20\ dB$ at $100\ Hz$	$29\ dB$
Steady state error	$<0.1\ \mu m$	$0\ \mu m$
Settling time	$< 1.5\ ms$	$1.151\ ms$
Closed-loop bandwidth	$> 1000\ Hz$	$1600\ Hz$
Gain margin	$> 5\ dB$	$8.4856\ dB$
Phase margin	$> 40\ deg$	$37.0338\ deg$
Max control action	$< 1.2\ V$	$0.735\ V$
Overshoot	< 20 %	41.367 %

Table 11: Specifications due to PID controller.

And the following results:

- *Disturbance error*: 32.4756 %
- *Noise error*: 1.1213 %

All the specifications are respected, but overshoot and phase margin.

6 Controllers comparison

In this section a comparison between the four designed controllers is presented.

6.1 Frequency response of the controllers

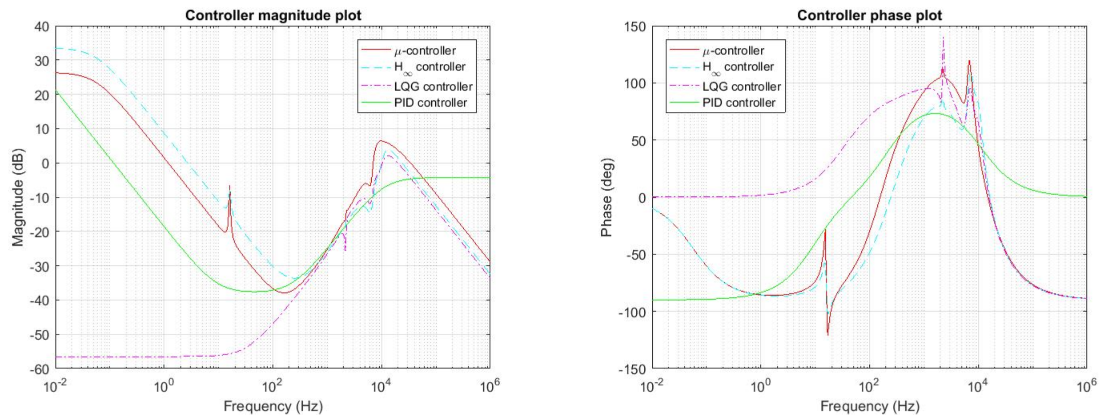

(a) Controller magnitude.

(b) Controller phase.

Figure 18: Comparison of the controllers frequency response.

6.2 Frequency response of the closed-loop systems

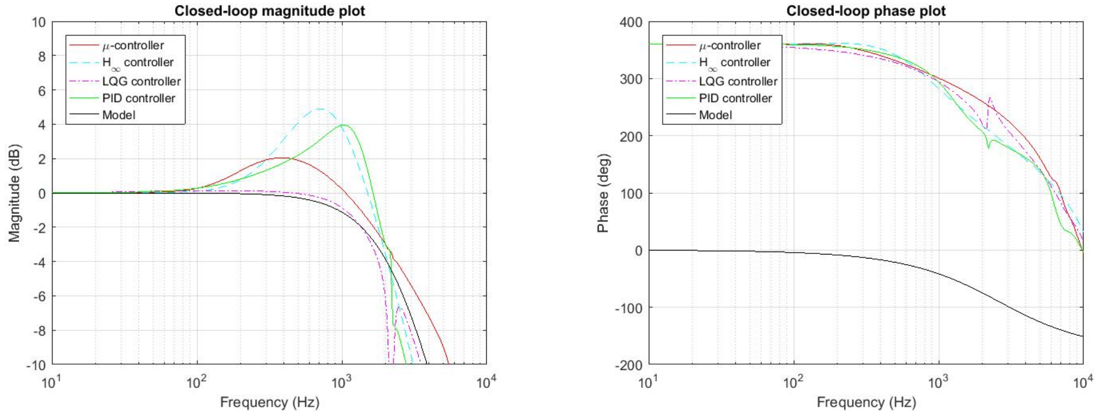

(a) Closed-loop magnitude.

(b) Closed-loop phase.

Figure 19: Comparison of the frequency closed-loop systems.

All closed-loop systems generate a frequency response near to that one of the ideal model.

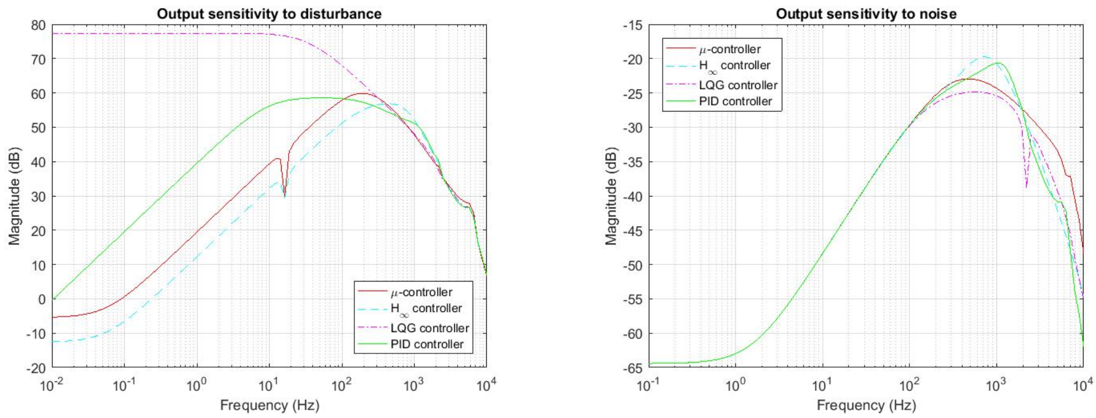

(a) Output sensitivity to disturbance.

(b) Output sensitivity to noise.

Figure 20: Comparison of the output sensitivities.

6.3 Transient response of the closed-loop systems

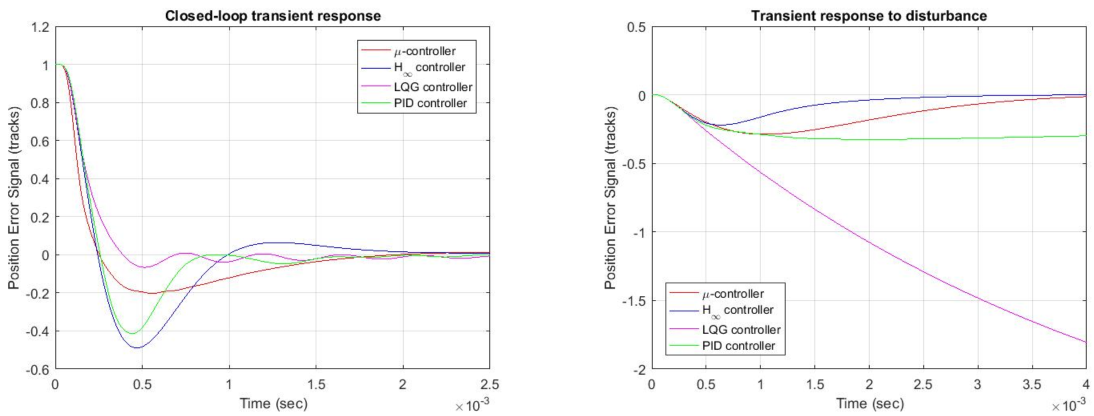

(a) Closed-loop transient response.

(b) Transient response to disturbance.

Figure 21: Comparison of the transient responses of the closed-loop systems.

All the closed-loop systems follow the reference. Only the *LQG* controller is not able to reject the disturbance.

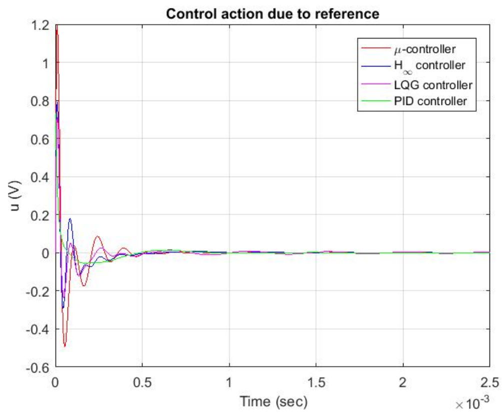

(a) Control action due to reference.

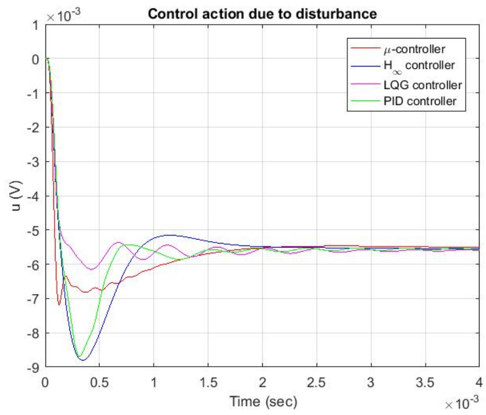

(b) Control action due to disturbance.

Figure 22: Comparison of the control actions.

Both control actions due to reference and disturbance are bounded and do not exceed the maximum admissible value.

6.4 Nominal Performance

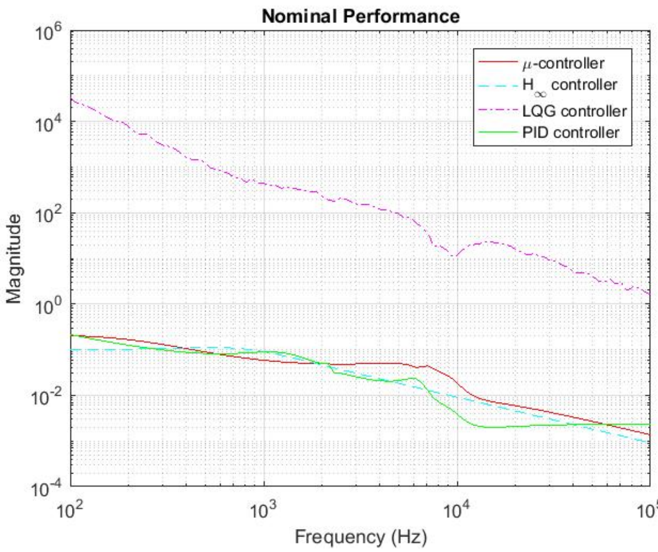

Figure 23: Nominal performance of the closed-loop systems.

NP is guaranteed by all controllers, but *LQG*.

6.5 Robust Stability

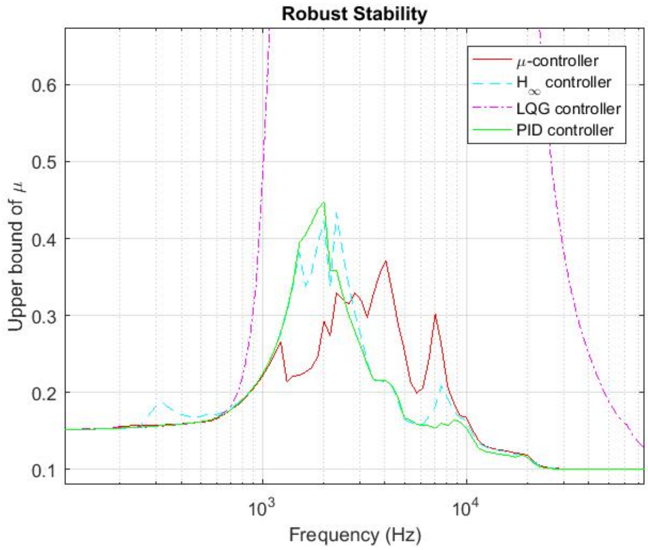

Figure 24: Robust stability of the closed-loop systems.

RS is guaranteed by all controllers, but *LQG* as expected since its standard formulation is not robust.

6.6 Robust Performance

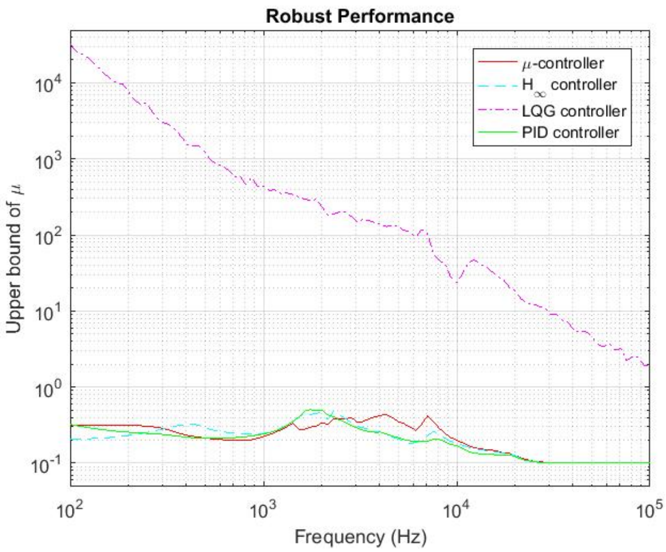

Figure 25: Robust performance of the closed-loop systems.

RS is guaranteed by all controllers, but *LQG*.

7 GUI

A *Graphic – User – Interface* (GUI) has been implemented in Matlab. It is shown in Figure 26.

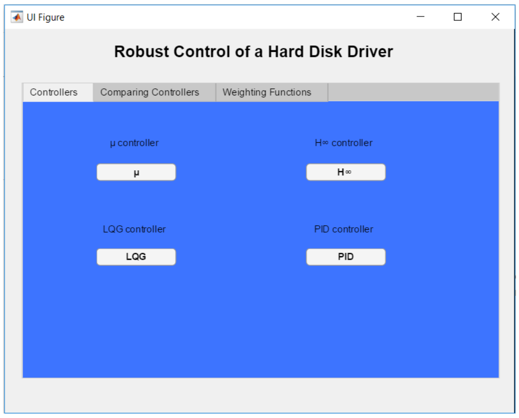

Figure 26: Graphic User Interface.

There are three tabs that can be accessed by the user:

- **Controllers**: the relative button generates the controller and useful graphics;
- **Comparing controllers**: all the graphics described in the section *Controllers comparison* can be displayed;
- **Weighting Functions**: graphics of the weighting functions can be displayed.

A Matlab files

Here a description for each Matlab file is presented.

- **cfr_hdd.m**: Closed-loop frequency response with all controllers.
- **clp_hdd.m**: Transient responses of the closed-loop system.
- **contents.m**: A list with description for each file.
- **ctr_hdd.m**: Transient responses of all closed-loop systems.
- **dk_hdd.m**: Sets the DK-iterations parameters in the μ-synthesis.
- **frs_hdd.m**: Frequency responses of the closed-loop system.
- **gui_hdd.mlapp**: Run the GUI.
- **hinf_hdd.m**: Design of H_∞ controller.
- **kf_hdd.m**: Frequency responses of all controllers.
- **lqg_hdd.m**: Design of LQG controller.
- **mod_hdd.m**: Creates the uncertainty system model.
- **model_hdd.m**: Generates the ideal model.
- **ms_hdd.m**: Design of μ-controller.
- **mu_hdd.m**: Analysis of robust stability, nominal and robust performance.
- **olp_hdd.m**: Creates the model of the uncertain open-loop system.
- **pid_hdd.m**: Design of PID controller.
- **prf_hdd.m**: Nominal performance of the four closed-loop systems.
- **rbp_hdd.m**: Robust performance of the four closed loop systems.
- **rbs_hdd.m**: Robust stability of the four closed loop systems.
- **sim_hdd.m**: Creates the simulation model of the closed loop system.
- **weights_hdd.m**: Generates the weighting functions.